AALBORG UNIVERSITY

DENMARK

Zero-tail DFT-spread-OFDM signals

Berardinelli, Gilberto; Tavares, Fernando Menezes Leitão; Sørensen, Troels Bundgaard; Mogensen, Preben; Pajukoski, Kari

Zero-tail DFT-spread-OFDM signals

Gilberto Berardinelli [(1)], Fernando M. L. Tavares [(1)], Troels B. Sørensen [(1)],
Preben Mogensen [(1)(2)], Kari Pajukoski [(3)]

[(1)] Department of Electronic Systems, Aalborg University, Denmark
[(2)] Nokia Solutions and Networks, Aalborg, Denmark
[(3)] Nokia Solutions and Networks, Oulu, Finland

Abstract—In the existing scheduled radio standards using Orthogonal Frequency Division Multiplexing (OFDM) or Discrete Fourier Transform-spread-OFDM (DFT-s-OFDM) modulation, the Cyclic Prefix (CP) duration is usually hard-coded and set as a compromise between the expected channel characteristics and the necessity of fitting a predefined frame duration. This may lead to system inefficiencies as well as bad coexistence with networks using different CP settings. In this paper, we propose the usage of zero-tail DFT-s-OFDM signals as a solution for decoupling the radio numerology from the expected channel characteristics. Zero-tail DFT-s-OFDM modulation allows to adapt the overhead to the estimated delay spread/propagation delay. Moreover, it enables networks operating over channels with different characteristics to adopt the same numerology, thus improving their coexistence. An analytical description of the zero-tail DFT-s-OFDM signals is provided, as well as a numerical performance evaluation with Monte Carlo simulations. Zero-tail DFT-s-OFDM signals are shown to have approximately the same Block Error Rate (BLER) performance of traditional OFDM, with the further benefit of lower out-of-band (OOB) emissions.

I. INTRODUCTION

Orthogonal Frequency Division Multiplexing (OFDM) modulation is a cost-effective solution for coping with large delay spread channels and has been adopted by several radio standards, from IEEE 802.11 [1] to Long Term Evolution (LTE) and Long Term Evolution - Advanced (LTE-A) [2]. The attractiveness of OFDM is mainly due to its capability of converting the frequency selective channel to multiple flat channels, enabling simple one-tap equalization at the receiver [3]. Discrete Fourier Transform -spread- OFDM (DFT-s-OFDM) is a straightforward *add on* over OFDM allowing to emulate a single carrier modulation with significant advantages in terms of power efficiency [4]. The effectiveness of both OFDM and DFT-s-OFDM in mitigating the fading is made possible through the insertion of a Cyclic Prefix (CP) at the beginning of each time symbol, obtained as a copy of the last part of the symbol itself. In case the CP length is larger than the delay spread of the channel, intersymbol interference is avoided and the signal is seen as cyclic at the receiver. This means, in the frequency domain the subcarriers where the data symbols are mapped are still orthogonal and efficient frequency domain processing can be applied [3].

However, the usage of the CP in an OFDM-based radio standard leads to significant limitations in the system design. First of all, the CP length must be hard-coded in order to fit with the frame duration, which is set according to upper layer requirements (e.g., latency). For instance, in LTE two different subframe structures have been defined: short CP of 4.7 μs with 14 time symbols and long CP of 8.6 μs with 12 time symbols, both fitting the constraint of 1 ms subframe duration [4]. This may lead to unnecessary throughput limitations in case the effective delay spread is significantly lower than the CP duration. On the contrary, it may affect the block error rate (BLER) performance in case such length is not sufficient to cope with a large delay spread. The option of using an adaptive CP, where its length is set with fine granularity according to the estimated channel, is unfeasible in practical scheduled systems due to the aforementioned constraint on the fixed frame duration. Moreover, the usage of different numerologies (e.g., LTE with long CP and short CP) may strongly affect the performance of different networks operating in proximity, since they would generate mutual asynchronous interference which cannot be canceled by computationally feasible receivers.

In this paper, we propose the usage of zero-tail DFT-s-OFDM signals as an alternative to traditional CP-based OFDM/DFT-s-OFDM modulation. Such signals are designed with the aim of decoupling the radio numerology from the channel characteristics by replacing the CP with a set of very low power samples (zero-tail) which are part of the Inverse Fast Fourier Transform (IFFT) output. This leads to the possibility of setting the overhead represented by the low power samples according to the estimated channel without compromising the numerology. Note that the proposed solution is different from known zero-padded approaches (e.g., [5], [6]), which replace the CP with zeros with the aim of improving robustness to the channel fades with a penalty in receiver complexity, since cyclicity at the receiver is partly lost. We aim instead at a solution which preserves the orthogonality of the data subcarriers at the receiver. The generation of a zero-word at the tail of the signal is also addressed by the unique word technique (e.g., [7], [8]), where the zero-tail is then replaced by deterministic sequences used for channel estimation or synchronization purposes. However, the zero-word is there obtained by precoding a set of redundant subcarriers with a complex matrix for each symbol. This may significantly increase the computational complexity. Our approach has instead approximately the same complexity as a LTE transceiver.

The paper is structured as follows. The motivations for the usage of zero-tail signal is given in Section II, while in Section III the signal generation is described. Section IV presents a theoretical analysis of the zero-tail DFT-s-OFDM signals. Simulation results are presented in Section V. Finally, Section VI resumes the conclusions and states the future work.

II. MOTIVATION FOR ZERO-TAIL SIGNALS

In a traditional OFDM/DFT-s-OFDM system, the CP duration T_{CP} is set according to the following requirement [3]:

$$T_{CP} \geq \tau_D + 2\tau_P \qquad (1)$$

where τ_D is the delay spread of the channel and τ_P is the propagation delay between transmitter and receiver. In case the condition in Eq.(1) is satisfied, the cyclicity of the signal at the receiver is preserved and simple one-tap equalization can be applied. Note that in LTE/LTE-A the propagation delay can be compensated by a timing advanced procedure [4], and the CP is mainly meant for coping with the delay spread.

As mentioned in the introduction, in the existing scheduled radio standards the CP length is hard-coded and is set as a compromise between overhead and estimation of the expected root mean square (RMS) delay spread in the intended environment (e.g., micro/macro cells). This inevitably leads to system inefficiency as well as bad coexistence with systems using a different CP length. With reference to Figure 1(a), two neighbor systems located in close proximity would generate indeed mutual asynchronous interference given their different CP settings, even when synchronized at frame level. Computationally feasible receivers such as Interference Rejection Combining (IRC) [9] or Successive Interference Cancellation (SIC) [10] can suppress synchronous interference but are not able to reject such asynchronous contribution, leading to poor link performance.

Let us consider now two frames containing OFDM/DFT-s-OFDM symbols without CP but with a certain set of zeros at their tail; with reference to Figure 1(b), different numbers of zeros can be set for two frames while preserving the same symbol duration. Let us assume that these zeros are not obtained by blanking the last samples of the IFFT, but can be generated as its natural output. In case the duration of the zero part T_{s_0} fulfills the same requirement of T_{CP} for Eq.(1), each OFDM/DFT-s-OFDM symbol does not spill its energy over the adjacent symbol, thus maintaining the signal cyclicity at the receiver. Such zero-tail signals have then the following advantageous properties:

1) Adaptivity to the estimated delay spread/propagation delay: T_{s_0} can be set dynamically without modifying the system numerology. This allows to avoid the potential throughput losses or BLER increase due to an hard-coded CP. Delay spread can be estimated for instance from pilot sequences periodically sent, and T_{s_0} set accordingly.
2) Coexistence with systems using different T_{s_0}. Since the T_{s_0} samples are part of the OFDM/DFT-s-OFDM symbol itself, systems operating over different types of channels can use the same numerology (e.g., symbol length). In case such systems are synchronized at both frame and symbol level, they can coordinate their transmission in order not to interfere each other. Moreover, even when simultaneously transmitting, they would generate mutual synchronous interference which can be suppressed by the aforementioned IRC
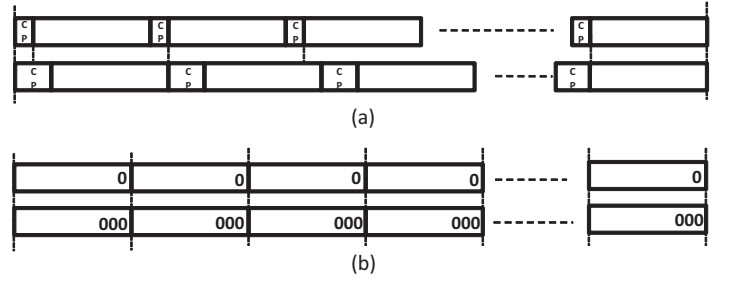

Fig. 1. CP-based signals (a) vs. zero-tail signals (b).

and SIC detectors, boosting the throughput performance.

Note that hybrid solutions are also possible, i.e. using a short CP and relying on the zero-tail for eventual longer propagation delay and delay spread. This may also enable coexistence with the current radio standards using traditional CP-based transmission.

III. ZERO-TAIL SIGNAL GENERATION

Zero-tail signals can be generated with a modified form of the traditional DFT-spread-OFDM chain [11]. Let us define the following $N \times 1$ column vector:

$$\mathbf{q} = \begin{bmatrix} \mathbf{0}_{N_h} & \mathbf{d}^T & \mathbf{0}_{N_t} \end{bmatrix}^T \qquad (2)$$

where $\mathbf{0}_x$ denotes a vector of zeros having length x, $\mathbf{d}$ is a $(N - N_h - N_t) \times 1$ column vector of data symbols, and $(\cdot)^T$ denotes the transpose operator. $\mathbf{q}$ is fed to the DFT block, whose output is then mapped over the frequency subcarriers and IFFT-processed. The resultant $N_{IFFT} \times 1$ time signal column vector $\mathbf{s}$ can be then expressed as:

$$\mathbf{s} = \frac{1}{\sqrt{N_{IFFT}(N - N_t - N_h)}} \mathbf{F}_{N_{IFFT}}^{-1} \mathbf{M} \mathbf{F}_N \mathbf{q} \qquad (3)$$

where $\mathbf{F}_P$ denotes the $P \times P$ unnormalized FFT matrix, i.e.

$$\mathbf{F}_P[a, b] = e^{-\frac{j2\pi ab}{P}} \qquad (4)$$

for $a = 0, \cdots, P - 1$, $b = 0, \cdots, P - 1$ and $\mathbf{M}$ is the $N_{IFFT} \times N$ matrix which maps the data on the frequency subcarriers (subcarrier mapping matrix). It can be shown that, by applying Eq.(3) on the input vector $\mathbf{q}$, the data symbol at position z concentrates most of its energy in the position $\lfloor z N_{IFFT}/N \rfloor$ of the time domain $\mathbf{s}$ vector [12], where $\lfloor x \rfloor$ denotes the nearest integer number higher than x. As a consequence, the pre-DFT vectors $\mathbf{0}_{N_h}$ and $\mathbf{0}_{N_t}$ will be spread over the beginning and the tail of $\mathbf{s}$. The length of the $\mathbf{s}_h$ and $\mathbf{s}_t$ vectors, representing the corresponding time domain zero-head and the zero-tail of $\mathbf{s}$, is given by, respectively:

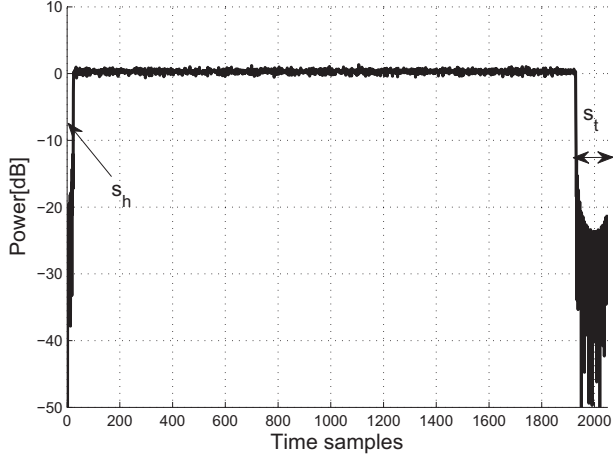$$N_{s_h} = \left\lfloor \frac{N_h N_{IFFT}}{N} \right\rfloor \qquad (5)$$

Fig. 2. Snapshot of a zero-tail DFT-s-OFDM signal. assuming $N = 1200$, N_{IFFT}=2048, N_{s_h}=17 and N_{s_t}=144.

$$N_{s_t} = \left\lfloor \frac{N_t N_{IFFT}}{N} \right\rfloor \qquad (6)$$

In Figure 2, a realization of the generated time domain signal is depicted, and the $\mathbf{s}_h$ and $\mathbf{s}_t$ vectors highlighted. It can be noticed that their power is not zero but considerably lower than the average transmit power. Such non-zero low power tail is due to the leakage of the data mapped over the rest of the time samples. N_{s_t} has to be designed to cope with the requirements of Eq.(1), while $\mathbf{s}_h$ only aims at ensuring that the IFFT cyclicity does not generate a power-regrowth at the very last samples of the tail, and it represents a further overhead of the zero-tail DFT-s-OFDM signals. The impact of such overhead will be discussed in the following sections. Note that N_t can be derived from Eq.(6) according to the N_{s_t} requirement.

In case of ideal unitary channel response, the transmit vector $\mathbf{q}$ can be retrieved as:

$$\mathbf{q} = \sqrt{N_{IFFT}(N - N_t - N_h)}\mathbf{F}_N^{-1}\mathbf{M}^{-1}\mathbf{F}_{N_{IFFT}}\mathbf{r} \quad (7)$$

where $\mathbf{r} = \mathbf{s}$ denotes the received signal, and the original data vector is then given by:

$$\mathbf{d} = \mathbf{q}\left[N_h : (N - N_t - 1)\right] \qquad (8)$$

With transmission over a fading channel, frequency domain equalization can be applied as in traditional OFDM and DFT-s-OFDM systems.

Note that the described zero-tail DFT-s-OFDM signal generation leads to traditional DFT-s-OFDM by setting $N_h = N_t = 0$; since the operations in Eq.(2) and Eq.(8) are trivial, the complexity of the zero-tail DFT-s-OFDM transceiver is the same as the traditional uplink LTE transceiver [4]. Moreover, the extension to Multiple-Input-Multiple-Output (MIMO) antenna transmission schemes is as straightforward as in any OFDM/DFT-s-OFDM scheme. Unfortunately, as in traditional DFT-s-OFDM the data symbols are spread over the entire bandwidth, and this prevents the usage of frequency selective

scheduling or link adaptation [12]. However, the possibility of applying frequency selective algorithms can be kept in case the DFT-spreading is applied, for instance, on a frequency resource block basis rather than on the entire bandwidth. This is for further studies.

It is worth to observe that the presence of both a zero-head and a zero-tail smoothens the abrupt transitions between adjacent time symbols; this is expected to reduce the Out-Of-Band (OOB) emissions of the signals with respect to baseline OFDM/DFT-s-OFDM.

Nonetheless, the transmitter chain described in this section generates signals having low but non-zero power at their tail and head, while the system benefits described in Section II subsume instead ideal zero-tail signals. The rest of the paper will address the impact of such non-ideal zero-tail on the performance.

IV. THEORETICAL ANALYSIS

In this section, a theoretical analysis of the zero-tail DFT-s-OFDM signals is provided.

Let us denote with N_{s_0} the total length of the time domain zero-part, i.e. $N_{s_0} = N_{s_h} + N_{s_t}$. For the sake of simplicity, without loss of generality, we assume that $N_{s_h} = 0$ and we only focus on the generation of $\mathbf{s}_t$.

Let us define the following $N_{IFFT} \times N$ matrix:

$$\vartheta = \frac{1}{\sqrt{N_{IFFT}(N - N_t)}}\mathbf{F}_{N_{IFFT}}^{-1}\mathbf{M}\mathbf{F}_N \qquad (9)$$

The time domain vector $\mathbf{s}$ can be then rewritten as:

$$\mathbf{s} = \vartheta\mathbf{q} \qquad (10)$$

$\mathbf{s}_t$ can be obtained as:

$$\mathbf{s}_t = \tilde{\vartheta}\mathbf{d} \qquad (11)$$

where $\tilde{\vartheta}$ represents the following partition of the ϑ matrix:

$$\tilde{\vartheta} = \vartheta\left(N_{IFFT} - N_{s_t} : N_{IFFT} - 1, 0 : N - N_t - 1\right) \quad (12)$$

The vector of the average power of $\mathbf{s}_t$ is then given by:

$$\mathbf{p}_{s_t} = E\left\{diag\left(\mathbf{s}_t\mathbf{s}_t^H\right)\right\} = E\left\{diag\left(\tilde{\vartheta}\mathbf{d}\mathbf{d}^H\tilde{\vartheta}^H\right)\right\} \quad (13)$$

where $E\{\cdot\}$ denotes the expectation operation, $(\cdot)^H$ is the hermitian operator and $diag(\cdot)$ returns the diagonal of the matrix where it is applied. Since the only random term in Eq.(13) is given by the data vector $\mathbf{d}$, it can be rewritten as follows:

$$\mathbf{p}_{s_t} = diag\left(\tilde{\vartheta}E\left\{\mathbf{d}\mathbf{d}^H\right\}\tilde{\vartheta}^H\right) \qquad (14)$$

Traditional data symbol constellations are defined in a way that their average power is unitary, i.e. $E\left\{\mathbf{d}\mathbf{d}^H\right\} = \mathbf{I}_{N-N_t}$,
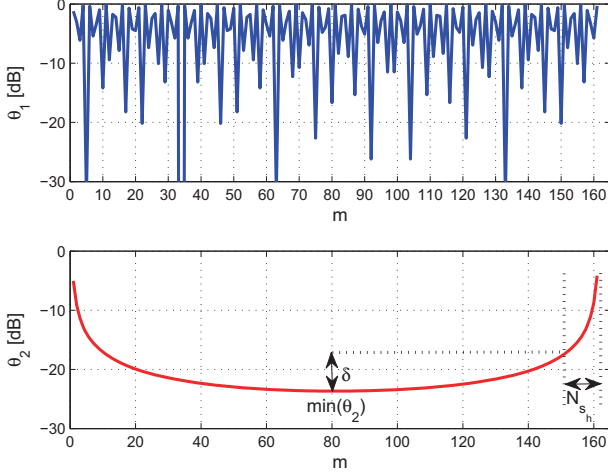
Fig. 3. Oscillating part and envelope of the zero-tail, assuming N=1200, N_{IFFT}=2048 and N_{s_t}=161.

Fig. 4. Zero-head overhead.

where $\mathbf{I}_P$ denotes the $P \times P$ identity matrix. The elements of $\mathbf{p}_{s_t}$ can be then expressed as:

$$p_m = |\mathbf{s}_t(m)|^2 = \sum_{k=0}^{N-N_t-1} \left| \tilde{\vartheta}(m,k) \right|^2 \qquad (15)$$

for $m = 0 : N_{s_t} - 1$. It can by shown by straightforward calculations that Eq.(15) can be expressed as the product of two independent functions:

$$p_m = \theta_1(m)\,\theta_2(m) \qquad (16)$$

with

$$\theta_1(m) = sin^2\left(\frac{\pi N(m + N_{IFFT} - N_{s_t})}{N_{IFFT}} \right) \qquad (17)$$

$$\theta_2(m) = \frac{1}{N^2} \sum_{k=0}^{N-N_t-1} csc^2\left(\frac{\pi(m + N_{IFFT} - N_{s_t})}{N_{IFFT}} - \frac{\pi k}{N} \right) \qquad (18)$$

Both θ_1 and θ_2 functions are displayed in Figure 3. θ_1 represents the oscillating part of the tail, while θ_2 is its envelope, and therefore represents the non-ideality of the zero-tail. θ_2 is a convex function and is nearly symmetrical with respect to its minimum. The power regrowth at the last samples is due to the cyclicity of the IFFT which appears in Eq.(9). By placing a zero-vector $\mathbf{0}_{N_h}$ at the beginning of the data vector, the last N_{s_h} samples of θ_2 are shifted to the beginning, as in Figure 2. As mentioned in Section III, $\mathbf{0}_{N_h}$ represents pure overhead and its length should be minimized. N_{s_h} can be parametrized as follows (see Figure 3(b)):

$$N_{s_h} = N_{s_0} - \theta_2^{-1}\left(min(\theta_2) + \delta \right) \qquad (19)$$

where δ represents the acceptable offset of power regrowth with respect to the minimum of the θ_2 function, and f^{-1} stands
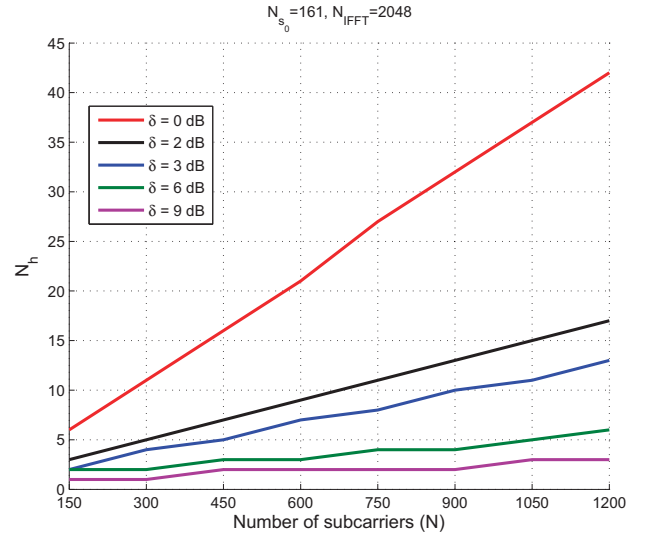
here for the inverse of the function f. Figure 4 shows the overhead of N_h as a function of the total number of data subcarriers, assuming N_{IFFT}=2048, for different values of δ. Obviously, N_h decreases with the increase of δ; a shorter zero-head is needed in case larger power regrowth can be tolerated. Note that the slope of the curves decreases with δ; this means, a smaller relative overhead is needed for large bandwidth allocations to achieve a certain power suppression. The impact of different power suppression levels on the link performance will be evaluated in the next section.

V. SIMULATION RESULTS

In this section, we evaluate numerically the performance of zero-tail DFT-s-OFDM by Monte Carlo simulations. Results are compared with traditional OFDM and DFT-s-OFDM modulations. Different zero-head sizes, parametrized as a function of the power suppression parameter δ, are considered. The main simulation parameters are gathered in Table 1. OFDM and DFT-s-OFDM are evaluated according to the traditional LTE numerology with short CP [4]. For zero-tail DFT-s-OFDM, the duration of the zero-tail T_{s_t} is set to be equal to the CP in OFDM/DFT-s-OFDM. In order to ensure a fair comparison, the configurations for the three modulation schemes are set such that the same maximum throughput can be achieved in case $N_h = 0$. The presence of a zero-head ($N_h \neq 0$) generates by default a throughput penalty for zero-tail DFT-s-OFDM.

An analysis of the characteristics of the transmit signals is carried out first. Figure 5 shows the Complementary Cumulative Distribution Function (CCDF) of the Peak-to-Average Power Ratio (PAPR) of zero-tail DFT-s-OFDM, assuming 16QAM modulation. The performance of OFDM and DFT-s-OFDM is also included for the sake of comparison. It is well known from literature that DFT-s-OFDM exhibits lower PAPR than OFDM due to its *quasi*-single carrier nature [13]. This allows the transmit power amplifier to work with a lower back-off, with remarkable advantages in terms of power efficiency. Zero-tail DFT-s-OFDM introduces a PAPR penalty

TABLE I.   SIMULATION PARAMETERS

Carrier frequency	2 GHz
Sampling frequency	30.72 MHz
Subcarrier spacing	15 KHz
FFT size	2048
Used subcarriers	150 (2.5 MHz), 1200 (20 MHz)
Subframe duration	1 ms
Symbols per subframe	14 (OFDM/DFT-s-OFDM)
	15 (zero-tail DFT-s-OFDM)
CP length	5.2[a]/4.68[b]μs (OFDM/DFT-s-OFDM)
	0 (zero-tail DFT-s-OFDM)
T_{s_t}	0 (OFDM/DFT-s-OFDM)
	4.68 μs (zero-tail DFT-s-OFDM)
MIMO schemes	1x4
User speed	3 kmph
Channel estimation	ideal
Channel code	3GPP Rel.8 compliant Turbo code
	with basic rate 1/3
Turbo decoder iterations	8
Receiver scheme	MMSE

[a] First OFDM/DFT-s-OFDM symbol in a slot.
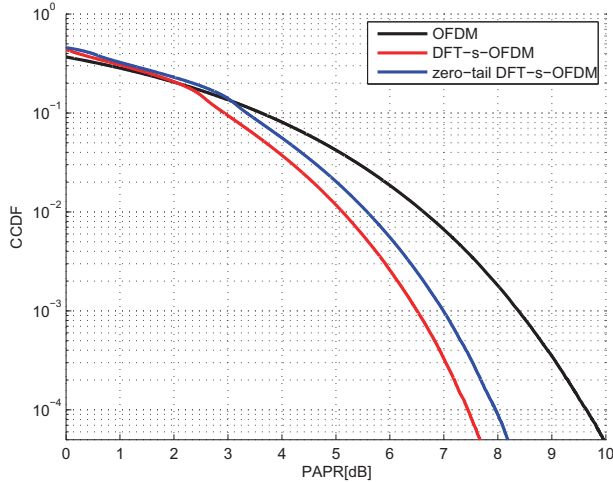[b] $2^{th} - 14^{th}$ OFDM/DFT-s-OFDM symbols in a slot.

Fig. 5.   PAPR performance of zero-tail DFT-s-OFDM, assuming 16QAM modulation.

of around 0.5 dB due to the presence of the low power samples in the tail. However, a considerable performance margin over OFDM is preserved. Such PAPR penalty can in principle be avoided by transmitting only the samples in the interval $(N_{s_h} : N_{IFFT} - N_{s_t} - 1)$, i.e. blanking with zeros the head and the tail of the signal; in this way, the power amplifier can be set to operate with the same back-off of DFT-s-OFDM. However, this option would modify the natural output of the IFFT and then introduce intercarrier interference. It is worth to notice that the PAPR penalty is dependent on the effective overhead of N_{s_h} and N_{s_t}, which can be reduced in case of channels with low estimated delay spread.

Figure 6 displays the Out-Of-Band (OOB) emissions of zero-tail DFT-s-OFDM, computed by using a Welch periodogram [14], assuming 1200 subcarriers configuration. When the zero-head is not added, zero-tail DFT-s-OFDM has approximately
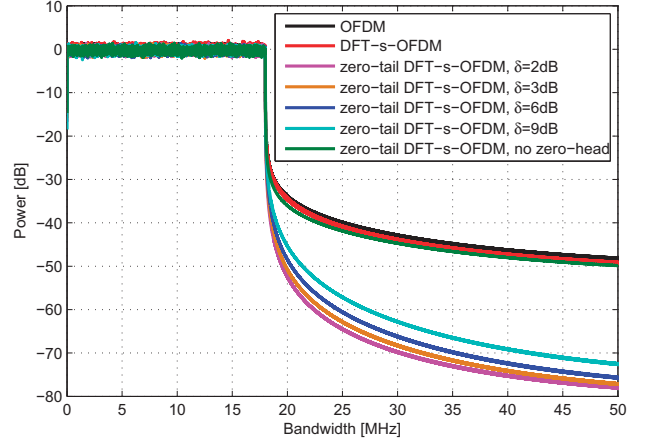
Fig. 6.   OOB emissions of zero-tail DFT-s-OFDM.

the same OOB emissions of OFDM/DFT-s-OFDM. However, the presence of the zero-head leads to significantly lower OOB emissions. This is due to the smooth transition between adjacent time symbols ensured by the low power samples at both the head and the tail of the signals. The OOB power regrowth due to high δ values is rather limited; an extremely short zero-head is sufficient for maintaining a low residual power on the adjacent bands. In this respect, zero-tail DFT-s-OFDM is particularly suited for cognitive radio applications [15], where the good spectral containment leads to an efficient usage of the available spectrum holes. Further, it also allows to increase the transmit power without significantly enhancing the interference on the adjacent channels. Note that, differently from known spectral shaping solutions such as raised cosine [16], the spectral containment of zero-tail DFT-s-OFDM does not come at the expense of signal distortion, but it is a inner property of the waveform itself.

The link performance evaluation is carried out by considering a typical urban channel model [17]. Data bits are encoded and interleaved according to the LTE Release 8 specifications [18]. We further assume full channel knowledge at the receiver and Minimum Mean Square Error (MMSE) equalization [11]. Single antenna transmission with 4 receive antennas is considered. The goal of the link level evaluation is to quantify the impact of the non-idealities of zero-tail DFT-s-OFDM. Figure 7 displays the BLER performance of the three considered modulations as a function of the Signal-to-Noise Ratio (SNR) for two different bandwidth configurations and assuming δ=3dB. DFT-s-OFDM has slightly higher BLER than OFDM. This is a consequence of the well known noise enhancement drawback of DFT-s-OFDM [11]: the presence of the IDFT in the receive chain spreads the noise contribution on the faded subcarriers over the whole bandwidth, thus affecting the BLER. Zero-tail DFT-s-OFDM achieves in general lower BLER than DFT-s-OFDM, thus performing closer to OFDM. This is because, at parity of average transmit power, zero-tail DFT-s-OFDM concentrates higher power on the data due to the presence of the samples with low energy, while in DFT-s-OFDM part of the power is lost in the CP. This allows to
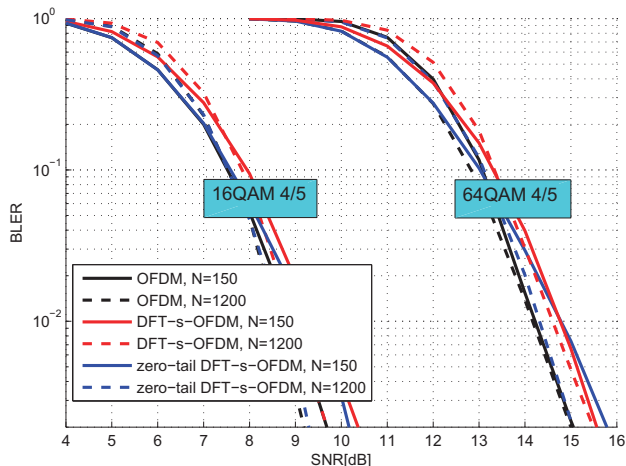
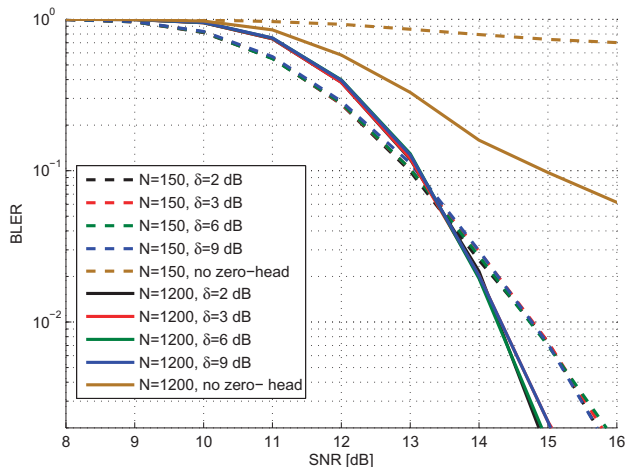Fig. 7. BLER performance of zero-tail DFT-s-OFDM, assuming δ= 3dB.

Fig. 8. BLER sensitivity of zero-tail DFT-s-OFDM to different zero-head sizes, assuming 64QAM 4/5.

partially compensate the noise enhancement, but at the expense of the aforementioned PAPR penalty. A slight degradation is only visible at high SNR region, which is however not significant when assuming for instance a typical BLER target of 10^{-1} as done in LTE [4].

The impact of different δ values, hence different N_h according to Eq.(19), is displayed in Figure 8 assuming 64QAM with coding rate 4/5 and different bandwidth configurations. It is clear that the usage of a zero-head is necessary for avoiding a disruptive performance, however, the BLER is fairly insensitive to the actual value of N_h. This suggests the possibility of using an extremely low overhead in zero-tail DFT-s-OFDM modulation without impacting the BLER.

VI. Conclusions and Future Work

In this paper we have proposed the usage of zero-tail DFT-s-OFDM signals as an alternative to traditional CP-based OFDM/DFT-s-OFDM transmission. Such signals replace the CP with a set of very low power samples which are obtained as a natural output of the IFFT at the transmitter. This allows

to adapt the signals to the estimated delay spread/propagation delay of the channel without affecting the system numerology. Moreover, it enables coexistence among systems designed for different environments (e.g., indoor/outdoor). Zero-tail signals have better spectral containment than OFDM/DFT-s-OFDM, and approximately the same link performance of OFDM with an extremely limited extra-overhead.

Future work is intended to address the system benefits of using zero-tail DFT-s-OFDM signals across networks having different delay spread requirements. Moreover, the aforementioned usage of frequency block - specific zero-tail DFT-s-OFDM is to be investigated. Finally, the proof-of-concept of zero-tail DFT-s-OFDM on a software defined radio testbed will be carried out.

References

[1] P. Roshan and J. Leary, *802.11 Wireless LAN Fundamentals*. Cisco Press, 2004.

[2] H. Holma and A. Toskala, *LTE-Advanced: 3GPP Solutions for IMT-Advanced*. Wiley, 2012.

[3] L. Hanzo, M. Munster, B. Choi, and T. Keller, *OFDM and MC-CDMA for Broadband MultiUser Communications, WLANs and Broadcasting*. John Wiley - IEEE Press, 2003.

[4] H. Holma and A. Toskala, *LTE for UMTS: OFDMA and SC-FDMA Based Radio Access*. Wiley, 2009.

[5] B. Muquet, Z. Wang, G. B. Giannakis, M. de Courville, and P. Duhamel, "Cyclic Prefixing or Zero Padding for Wireless Multicarrier Transmission," *IEEE Transactions on Communications*, vol. 50, no. 12, pp. 2136–2148, December 2002.

[6] P. D. Papadimitriou and C. N. Gheorghiades, "Zero-padded OFDM with improved performance over multipath channels," *International Conference in Communications, Circuits, and Systems*, pp. 727–731, 2008.

[7] M. Huemer, C. Hofbauer, and J. B. Huber, "The Potential of Unique Words in OFDM," *Proceedings International OFDM Workshop (in-OWo)*, pp. 140–144, 2010.

[8] C. Hofbauer, M. Huemer, and J. B. Huber, "Coded OFDM by unique word prefix," *IEEE International Conference on Communications Systems (ICCS)*, pp. 426–430, November 2010.

[9] M. Lampinen, F. Del Carpio, T. Kuosmanen, T. Koivisto, and M. Enescu, "System-level modeling and evaluation of itnerference suppression receivers in LTE systems," *Vehicular Technology Conference*, pp. 1–5, May 2012.

[10] H. Haykin, M. Sellathurai, Y. de Jong, and T. Willink, "Turbo-MIMO for wireless communications," *IEEE Communications Magazine*, vol. 42, no. 10, pp. 48–53, October 2004.

[11] B. E. Priyanto, H. Codina, S. Rene, T. B. Sørensen, and P. Mogensen, "Initial performance evaluation of DFT-spread OFDM based SC-FDMA for UTRA LTE Uplink," *IEEE 65th Vehicular Technology Conference, VTC2007-Spring*, pp. 3175–3179, April 2007.

[12] G. Berardinelli, *Air interface for next generation mobile communications networks: Physical Layer Design*. Ph.D. dissertation, Aalborg University, 2010.

[13] H. G. Myung, J. Lim, and D. J. Goodman, "Single carrier FDMA for uplink wireless transmission," *IEEE Vehicular Technology Magazine*, vol. 2, no. 3, pp. 30–38, September 2006.

[14] S. Salivahanan and A. Vallavaraj, *Digital Signal Processing*. Tata Mac-Graw Hill Education, 2001.

[15] S. Haykin, "Cognitive Radio: Brain-Empowered Wireless Communications ," *IEEE Journal on Selected Areas in Communications*, vol. 23, no. 2, pp. 201–220, February 2005.

[16] J. Proakis, *Digital Communications*, 4th edition. Mc-Graw Hill, 2001.

[17] "Deployment aspects," 3rd Generation Partnership Project, Tech. Rep. TR 25.943, V6.0.0, 2005.

[18] "Multiplexing and channel coding," 3rd Generation Partnership Project, Tech. Rep. TR 25.212, V8.0.0, November 2007.